# TRANSIENT STRESSES OF A FUNCTIONALLY GRADED PROFILE WITH TEMPERATURE-DEPENDENT MATERIALS UNDER THERMAL SHOCK

**Antonios M. Nikolarakis[1] and Efstathios E. Theotokoglou[2]**

[1,2] Department of Mechanics – Laboratory of Testing and Materials,
School of Applied Mathematical and Physical Science
National Technical University of Athens
Zografou Campus 15773, Athens, Greece
[1]e-mail: ant_nikola@yahoo.com
[2]e-mail: stathis@central.ntua.gr

**Keywords:** Thermal Barrier Coating, Functionally Graded Material, Finite Element Analysis, Temperature-Dependent.

**Abstract.** *The one-dimensional coupled problem of linear thermoelasticity of a Nickel-Zirconia functionally graded thermal barrier coating, subjected to uniform thermal shock conditions on its upper surface is considered. With the proposed analysis we intend to investigate numerically the effect of the type of distribution of the FGM's properties on the thermomechanical response of the Nickel-Zirconia profile. The thermomechanical properties of the materials are assumed temperature-dependent. The properties of the FGM layer are assumed to vary in the axial direction according to the sigmoid function. A finite element code is developed for the numerical analysis of the transient stress field resulting from the thermal shock at the upper surface of the configuration. Time integration of the problem is based on the Implicit Euler Method. A parametric study follows to optimize the type of distribution of the thermomechanical properties of the FGM layer, which minimizes the magnitude of the generated stress wave. The effect of the temperature-dependency of the materials' properties is also discussed.*

## 1 INTRODUCTION

Functionally Graded Materials (FGMs) are advanced materials that connect two different materials in composite configurations. Their properties vary gradually between the properties of those two materials. The continuous variation of their properties limits the magnitude of the local stress concentration at interfaces. FGMs are increasingly used in thermal barrier coatings [1-3].

Ceramic/FGM/Metal composite materials are commonly used as thermal coatings. In this contribution we investigate the thermomechanical response of a 3-layered Zirconia/FGM/Nickel half-space under thermal shock conditions. The governing equations are derived from the theory of fully coupled thermoelasticity. Under the assumption of plain strain conditions and uniform loading on the upper surface, the displacement and temperature fields become one-dimensional. The properties of the materials are considered temperature-dependent. Several studies have been made about the thermomechanical behavior of functionally graded materials under thermal shock [4-6]. The authors of this contribution have studied this problem in the case of materials with temperature-independent properties and linear distribution of the properties of the FGM layer [6]. In the case of temperature-dependent properties we have a more realistic model.

In this paper, the properties of the FGM layer vary from the properties of the Zirconia to the properties of Nickel according to the sigmoid function. A parametric study follows to numerically examine the effect of the spatial distribution of the properties inside the FGM layer. A Finite Element code is developed in Matlab [7] for the calculation of transient thermal stresses inside the configuration. The influence of the temperature-dependency of the thermomechanical properties of the materials is also discussed.

## 2 GOVERNING EQUATIONS AND NUMERICAL ANALYSIS

### 2.1 Equations of fully coupled thermoelasticity

Consider an elastic 3-layered Zirconia/FGM/Nickel half-space as shown in Figure 1 under thermal shock conditions. Initially, the configuration is undeformed, stress-free and has a uniform temperature $T_0$. Under the

assumption of temperature-dependent properties, the theory of fully coupled thermoelasticity leads to the following system of equations at a point with cartesian coordinates $\mathbf{x}$ and at time $t$ [8]:

$$\begin{aligned} \left(\lambda u_{j,j} - \beta\theta\right)_{,i} + \left[\mu\left(u_{i,j} + u_{j,i}\right)\right]_{,j} &= \rho\ddot{u}_i, \quad i, j = 1,2,3 \\ \left(k\theta_{,i}\right)_{,i} &= \rho c_v\dot{\theta} + \beta T_0\dot{u}_{i,i}, \quad i = 1,2,3 \end{aligned} \tag{1}$$

where $\lambda = \lambda(\mathbf{x},\theta)$ and $\mu = \mu(\mathbf{x},\theta)$ are the Lame constants, $u_i = u_i(\mathbf{x},t)$ are the components of the displacement vector, $\beta_{ij} = \beta_{ij}(\mathbf{x},\theta)$ is the thermal moduli tensor, $\theta = \theta(\mathbf{x},t)$ is the variation of temperature, $\rho = \rho(\mathbf{x},\theta)$ is the density of the material, $k_{ij} = k_{ij}(\mathbf{x},\theta)$ are the heat conduction coefficients and $c_v = c_v(\mathbf{x},\theta)$ is the specific heat capacity under constant volume. A comma indicates partial differentiation with respect to a spatial variable and a dot above a variable indicates differentiation with respect to time.

Under the assumptions of plain strain conditions and uniform loading the displacement field and the variation of temperature field become one-dimensional. Eqs (2) are simplified as follows:

$$\begin{aligned} \frac{\partial}{\partial x}\left[(\lambda + 2\mu)\frac{\partial u}{\partial x} - \beta\theta\right] &= \rho\frac{\partial^2 u}{\partial t^2} \\ \frac{\partial}{\partial x}\left(k\frac{\partial\theta}{\partial x}\right) &= \rho c_v\frac{\partial\theta}{\partial t} + \beta T_0\frac{\partial^2 u}{\partial x\partial t} \end{aligned} \tag{2}$$

where $x$ is the spatial variable along the thickness of the layers.

The $\sigma_{xx}$ component of the stress field is given by [8]:

$$\sigma_{xx} = (\lambda + 2\mu)\frac{\partial u}{\partial x} - \beta\theta \tag{3}$$

Subsequently, the velocity $v = v(x,t) \equiv \partial u / \partial t$ is introduced as a new depended variable and the following variables are introduced for normalization purposes:

$$\begin{aligned} \omega = \frac{c_w}{\kappa}x, \ \eta = \frac{c_w^{\,2}}{\kappa}t \\ \Theta = \frac{1}{T_0}\theta, \ V = \frac{1}{c_w}v, \ U = \frac{c_w}{\kappa}u \end{aligned} \tag{4}$$

where $c_w = \left(\sqrt{(\lambda + 2\mu)/\rho}\right)(x_N)$ is the elastic wave velocity, $\kappa = \left[k/(\rho c_v)\right](x_N)$ is the thermal diffusivity and $x_N$ is a reference point inside the Nickel layer.

Hence eqs (2) take the following normalized form:

$$\begin{aligned} \rho c_v\frac{\partial\Theta}{\partial\eta} &= \frac{1}{\kappa}\frac{\partial}{\partial\omega}\left(k\frac{\partial\Theta}{\partial\omega}\right) - \beta\frac{\partial V}{\partial\omega} \\ \rho\frac{\partial V}{\partial\eta} &= \frac{1}{c_w^{\,2}}\frac{\partial}{\partial\omega}\left[(\lambda + 2\mu)\frac{\partial U}{\partial\omega} - \beta T_0\Theta\right] \\ \frac{\partial U}{\partial\eta} &= V \end{aligned} \tag{5}$$

Due to the dependency of the thermomechanical properties on temperature, eqs (5) describe a nonlinear problem. The normalized form for the $\sigma_{xx}$ component of the stress field is given by:

$$S = \frac{\lambda + 2\mu}{\beta_N T_0}\frac{\partial U}{\partial\omega} - \frac{\beta}{\beta_N}\Theta \tag{6}$$

where $\beta_N = \beta(x_N)$.

### 2.2 Finite Element analysis and time integration

Application of the Finite Element Method [9] to eqs (5), using 2-node linear shape functions, leads to the variational formulation of the problem:

$$\begin{aligned}
&\int_{\omega_i}^{\omega_{i+1}} w_1 \rho c_v \frac{\partial \Theta}{\partial \eta} d\omega = \frac{1}{\kappa}\left\{ -\int_{\omega_i}^{\omega_{i+1}} \frac{\partial w_1}{\partial \omega} k \frac{\partial \Theta}{\partial \omega} d\omega + \left[ w_1 k \frac{\partial \Theta}{\partial \omega} \right]_{\omega_i}^{\omega_{i+1}} \right\} - \int_{\omega_i}^{\omega_{i+1}} w_1 \beta \frac{\partial V}{\partial \omega} d\omega \\
&\int_{\omega_i}^{\omega_{i+1}} w_2 \rho \frac{\partial V}{\partial \eta} d\omega = \frac{1}{c_w^{\,2}}\left\{ -\int_{\omega_i}^{\omega_{i+1}} \frac{\partial w_2}{\partial \omega} \left[ (\lambda + 2\mu) \frac{\partial U}{\partial \omega} - \beta T_0 \Theta \right] d\omega + \right. \\
&\qquad \left. + \left[ w_2 \left[ (\lambda + 2\mu) \frac{\partial U}{\partial \omega} - \beta T_0 \Theta \right] \right]_{\omega_i}^{\omega_{i+1}} \right\} \\
&\int_{\omega_i}^{\omega_{i+1}} w_3 \frac{\partial U}{\partial \eta} d\omega = \int_{\omega_i}^{\omega_{i+1}} w_3 V d\omega
\end{aligned} \tag{7}$$

where $w_1, w_2, w_3 \in H^1$ are the weight functions.

Based on eqs (7) the local matrix equation of a finite element is formed. The global matrix equation of the problem under consideration is constructed by summing up all the local elemental matrices:

$$\mathbf{C}\,\dot{\mathbf{y}} = \mathbf{K}\,\mathbf{y} + \mathbf{f} \tag{8}$$

where $\mathbf{C}$, $\mathbf{K}$ and $\mathbf{f}$ are derived from eqs (7) and $\mathbf{y}$ is the vector of the unknowns.

The Implicit Euler Method [10] is used for the time integration of eqn (8). Let $\mathbf{y}_n$ be the unknown vector at time step $n$. Then the Implicit Euler Method yields:

$$\mathbf{y}_{n+1} = \left(\mathbf{I} - t_h \mathbf{C}^{-1}\mathbf{K}\right)^{-1} \left(\mathbf{y}_n + t_h \mathbf{C}^{-1}\mathbf{f}\right) \tag{9}$$

where $t_h$ is the time step used.

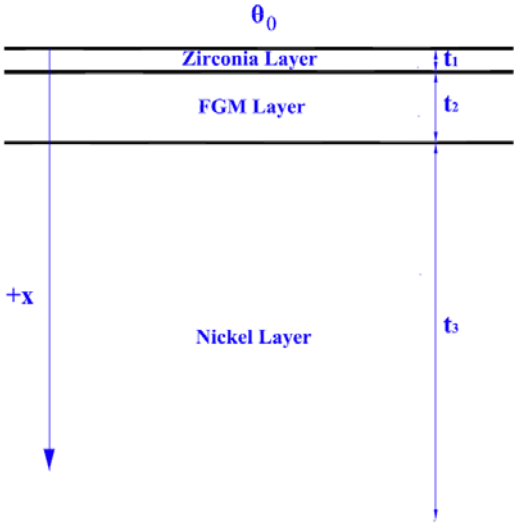


Figure 1: The 3-layered composite configuration under thermal shock conditions at the upper surface

## 3 RESULTS

### 3.1 Description of the problem

The 3-layered elastic half-space is initially at uniform temperature $T_0 = 300$ K. The normalized thickness of each layer is equal to $t_1 = 0.5$ for the Zirconia layer, $t_2 = 1.5$ for the FGM layer and $t_3 = \infty$ for the Nickel layer,

as shown in Figure 1. The thermomechanical properties of Zirconia and Nickel as a function of temperature $T$ are shown in Table 1 and 2 respectively [11]. At time $\eta = 0$ the normalized temperature of the upper surface of the half-space suddenly increases by $\Theta_0 = 1$. In the subsequent analysis, the distribution of the transient stress field is studied.

The problem described above is one-dimensional. A finite element code for the numerical analysis of eqn (8) is built in Matlab. The authors of this paper have tested the accuracy of the code in previous work [6]. Due to the nonlinear nature of the problem under consideration, the matrices $\mathbf{C}$ and $\mathbf{K}$ have to be recalculated at each time step. In the following applications, 2400 finite elements and 2000 time steps are used in order to ensure a satisfactory convergence.

| | |
|---|---|
| Density $\rho$ (kg·m$^{-3}$) | 4400 |
| Specific heat capacity $c_v$ (J·kg$^{-1}$·K$^{-1}$) | $1.71\cdot10^{-7}T^3 - 6.19\cdot10^{-4}T^2 + 7.95\cdot10^{-1}T + 308.093$ |
| Thermal conductivity $k$ (J·m$^{-1}$·K$^{-1}$·s$^{-1}$) | $0.116\cdot10^{-6}T^2 + 0.21\cdot10^{-3}T + 2.8936$ |
| Elasticity Modulus $E$ (GPa) | $-8.1\cdot10^{-6}T^2 - 50.3\cdot10^{-3}T + 65.819$ |
| Poisson's ratio $\nu$ | 0.25 |
| Thermal expansion coefficient $a$ ($10^{-6}$·K$^{-1}$) | $12.7\cdot10^{-6}T^2 - 18.9\cdot10^{-3}T + 13.527$ |

Table 1 : Thermomechanical properties of Zirconia

| | |
|---|---|
| Density $\rho$ (kg·m$^{-3}$) | 8900 |
| Specific heat capacity $c_v$ (J·kg$^{-1}$·K$^{-1}$) | $0.5023T + 302.022$ |
| Thermal conductivity $k$ (J·m$^{-1}$·K$^{-1}$·s$^{-1}$) | $1.876168\cdot10^{-7}T^3 - 2.126458\cdot10^{-4}T^2 + 2.717507\cdot10^{-2}T + 97.62$ |
| Elasticity Modulus $E$ (GPa) | $-1.508946\cdot10^{-5}T^2 - 4.161243\cdot10^{-2}T + 234.8317$ |
| Poisson's ratio $\nu$ | 0.30 |
| Thermal expansion coefficient $a$ ($10^{-6}$·K$^{-1}$) | $1.143460\cdot10^{-2}T + 9.5696$ |

Table 2 : Thermomechanical properties of Nickel

### 3.2 Distribution of the thermomechanical properties

The through thickness variation of the properties of the FGM layer is assumed to follow the sigmoid function in terms of parameter $p$ [12]. As a result of the temperature-dependency of the thermomechanical properties of Zirconia and Nickel, the distribution of the properties inside the half-space is not static. The expression for the modulus of elasticity as a function of depth $\omega$ and temperature $T$ is given by:

$$E(\omega,T) = \begin{cases} E_Z(T), & if\ 0 \le \omega \le t_1 \\ E_Z(T) + \left[E_N(T) - E_Z(T)\right]\dfrac{1}{2}\left[\dfrac{2(\omega - t_1)}{t_2}\right]^p, & if\ t_1 < \omega \le t_1 + \dfrac{t_2}{2} \\ E_Z(T) + \left[E_N(T) - E_Z(T)\right]\left\{1 - \dfrac{1}{2}\left[\dfrac{2(t_1 + t_2 - \omega)}{t_2}\right]^p\right\}, & if\ t_1 + \dfrac{t_2}{2} < \omega < t_1 + t_2 \\ E_N, & if\ \omega \ge t_1 + t_2 \end{cases} \tag{10}$$

where $E_Z(T)$ and $E_N(T)$ are the modulus of elasticity of Zirconia and Nickel respectively at temperature $T$. For $p = 1$ eqs (10) express the linear variation.

The expressions for the other thermomechanical properties are similar. In the numerical analysis the displacement, velocity and variation of temperature fields are derived at each time step. The distribution of the properties of Zirconia and Nickel are calculated based on equations of Table 1 and 2 and the variation of temperature field. The properties inside the FGM layer are then estimated according to eqs (10). Figures 2-4 show the distribution of selected thermomechanical properties for several values of the parameter $p$.

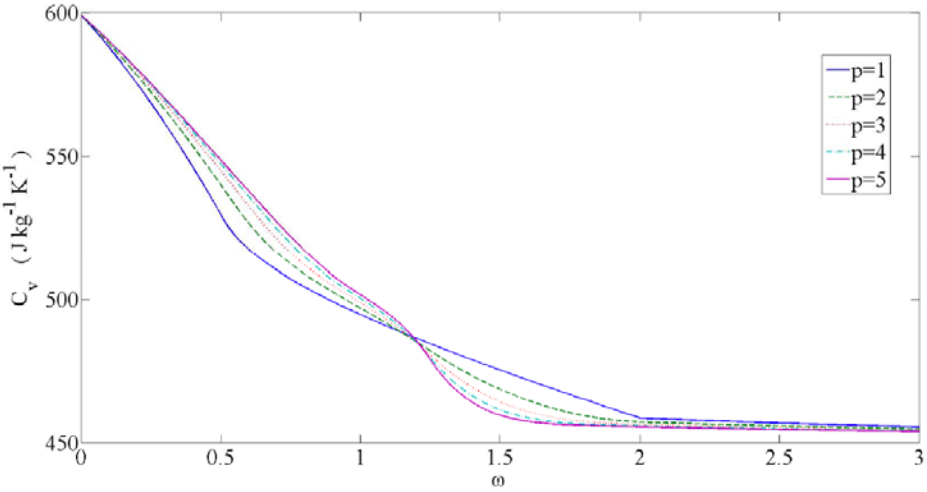


Figure 2: Distribution of the specific heat capacity at dimensionless time $\eta = 4$

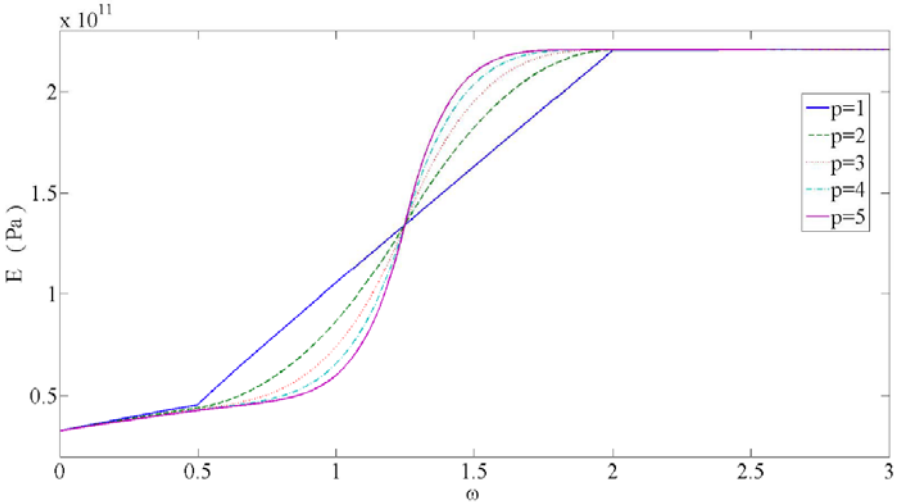


Figure 3: Distribution of the modulus of elasticity at dimensionless time $\eta = 4$

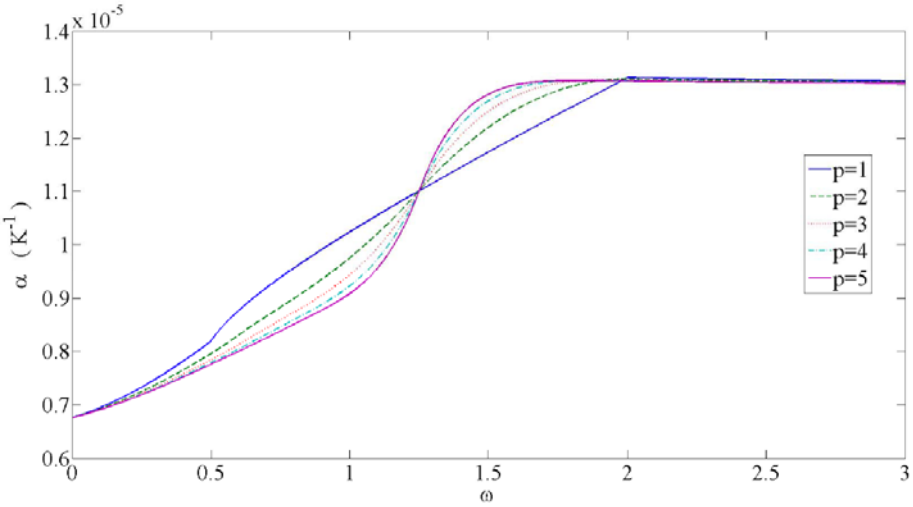


Figure 4: Distribution of the thermal expansion coefficient at dimensionless time $\eta = 4$

Figures 5-7 show the distribution of the same properties for $p = 3$ at various time points. The distribution at time $\eta = 0$ signifies the case of materials with temperature-independent properties. As time increases, the temperature inside the half-space rises. As a result, the specific heat capacity increases and the modulus of

elasticity decreases, Furthermore, the thermal expansion coefficient inside the Zirconia layer decreases and the thermal expansion coefficient inside the Nickel increases.

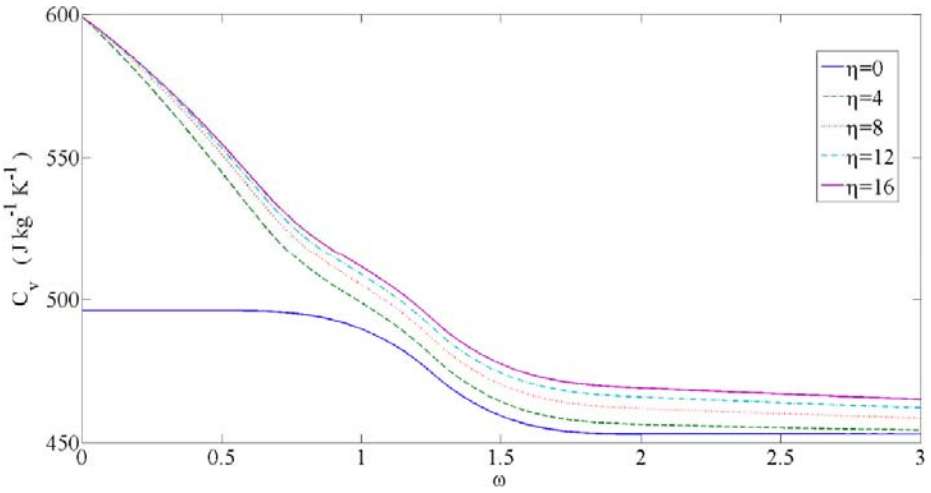


Figure 5: Distribution of the specific heat capacity for $p = 3$

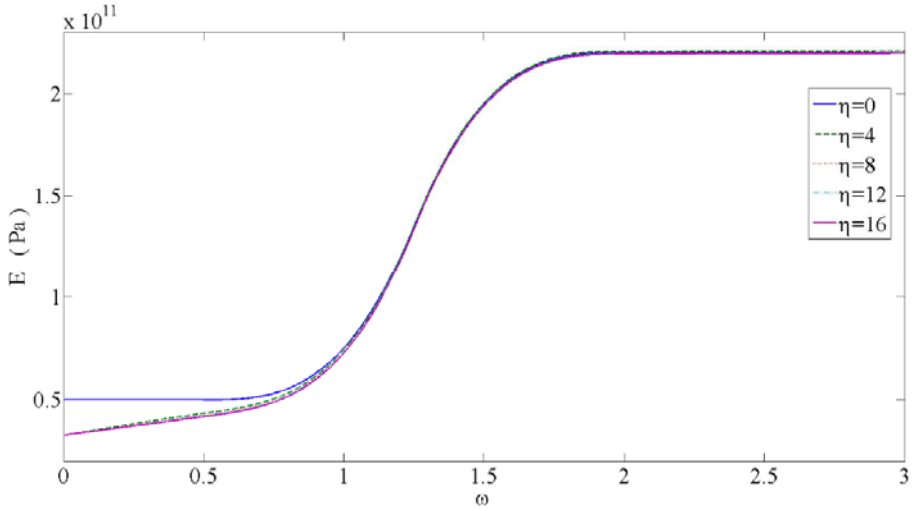


Figure 6: Distribution of the modulus of elasticity for $p = 3$

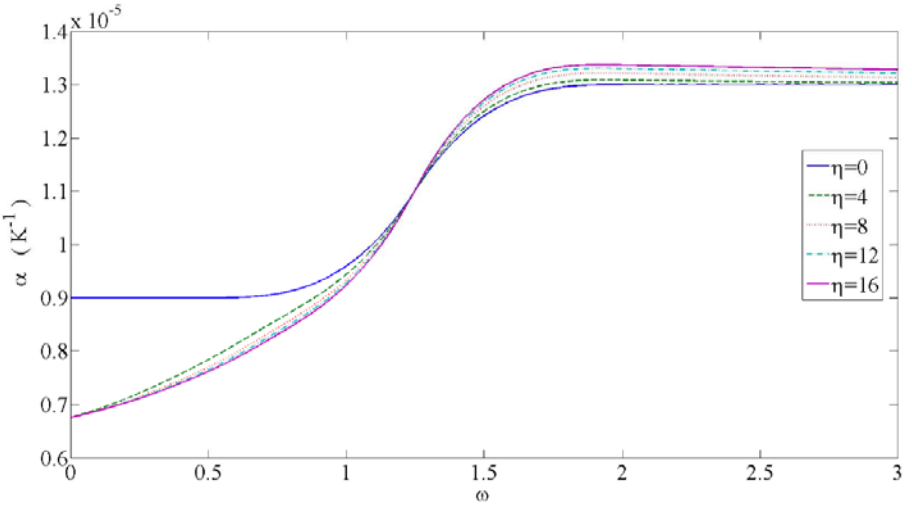


Figure 7: Distribution of the thermal expansion coefficient for $p = 3$

### 3.3 Transient stress field

Figures 8 and 9 show the time evolution of the normalized stress at position $\omega = 0.25$ and $\omega = 0.5$, respectively, for various values of the parameter $p$. The position $\omega = 0.25$ is located inside the Zirconia layer, while the position $\omega = 0.5$ is located at the interface between the Zirconia and the FGM layer. The two Figures show the main compressive stress wave that travels through the half-space, followed by less intense stress waves due to the reflection at the interface of between the Zirconia and the FGM layer and the upper surface. Zirconia, as a ceramic material, and the interfaces in general are susceptible to tension stresses and fatigue. Therefore, the criteria for the selection of the optimal type of distribution is the minimization of the intensity of the repeated tension waves at those two positions.

According to Figures 8 and 9, the generated tension waves are smoother when $p = 1$.

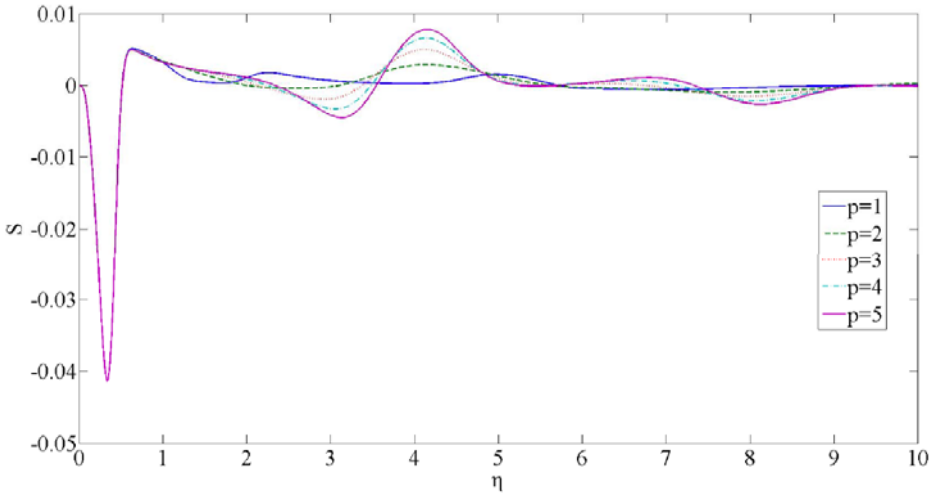


Figure 8: Time evolution of the normalized stress at dimensionless depth $\omega = 0.25$

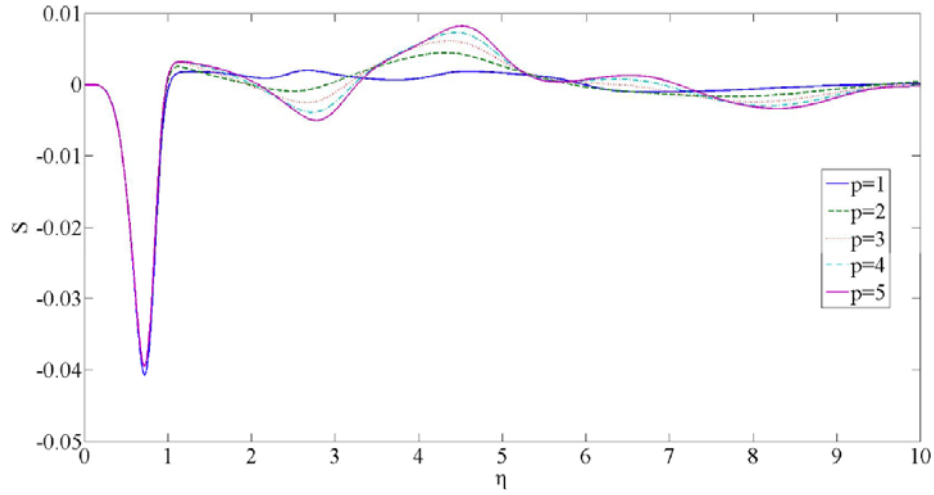


Figure 9: Time evolution of the normalized stress at dimensionless depth $\omega = 0.5$

### 3.4 Effect of the temperature-dependency of the thermomechanical properties

In this section we discuss the effect of the temperature-dependent properties on the magnitude of the generated waves. Figures 10 and 11 show the time evolution of the normalized stress at position $\omega = 0.25$ and $\omega = 0.5$, respectively, when $p = 1$ and for the cases of temperature-dependent and temperature-independent properties. It is clear that the assumption of materials with temperature-independent properties leads to conservative results, since the calculated magnitude of the initial stress wave is overvalued by approximately 30%. That is expected, since the modulus of elasticity of the materials with temperature-dependent properties is reduced, thus resulting in "softer" materials. It is concluded that when the temperature-dependency of the thermomechanical properties of the materials is not taken into account, the thermal shock resistance of the configuration is underestimated.

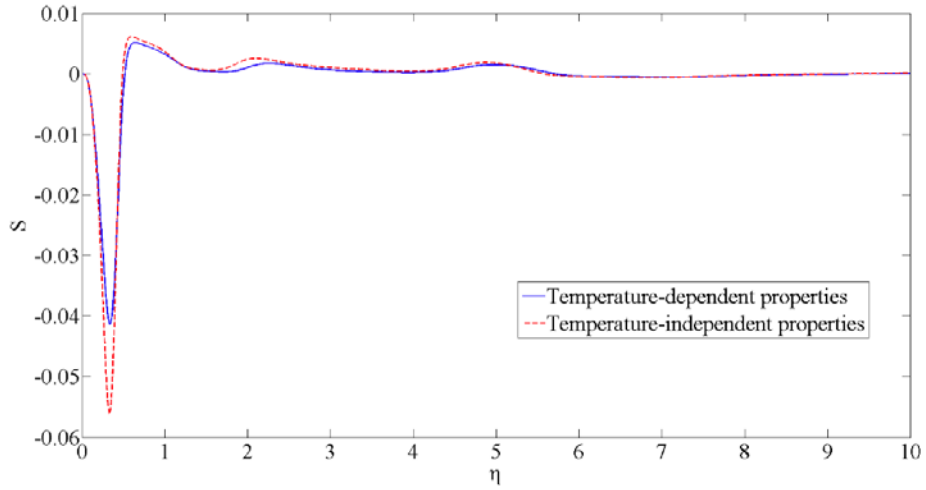


Figure 10: Time evolution of the normalized stress for $p=1$, at dimensionless depth $\omega=0.25$

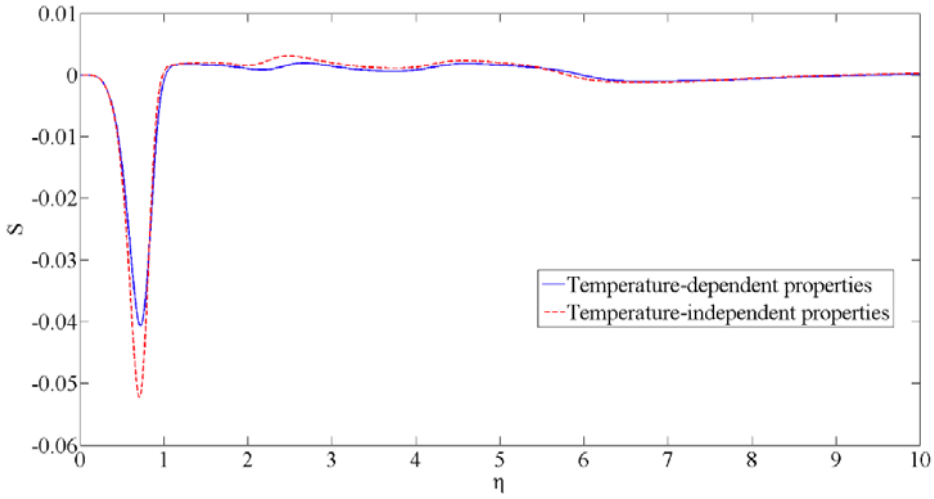


Figure 11: Time evolution of the normalized stress for $p=1$, at dimensionless depth $\omega=0.5$

## 4 CONCLUSIONS

In the this contribution, the one-dimensional problem of coupled thermoelasticity of a 3-layered Zirconia-FGM-Nickel half-space subjected to uniform thermal shock boundary conditions on the upper surface is studied numerically. The partial differential equations that describe the problem are presented and the finite element method with linear 2-node shape functions is applied, resulting in a ordinary differential equation system with respect to time. The Implicit Euler method is used for the time integration of the resulting system. A matlab finite element code is used for the numerical analysis of the problem described above and the calculation of the generated stresses. The materials of the half-space are assumed to have temperature-dependent thermomechanical properties, thus the problem under investigation is nonlinear. The properties of the FGM layer are assumed to vary in the axial direction according to the sigmoid function with parameter $p$.

A parametric study shows that the reflected tension stress waves are inside the Zirconia layer and at the interface Zirconia/FGM are minimized for $p=1$. This is important for composite thermal coatings with ceramic/metal materials, due to the vulnerability of the ceramic material and to tensile stresses and fatigue. A comparative study also indicates that the assumption of temperature-independent properties is conservative: when the effect of temperature on the thermomechanical properties of the materials is taken into account, the calculated maximum compressive stress is reduced by 30%.

**ACKNOWLEDGMENT**

The first author of this paper was financially supported for his contribution by the IKY FELLOWSHIPS OF EXCELLENCE FOR POSTGRADUATE STUDIES IN GREECE - SIEMENS PROGRAM, as part of his Ph.D. Thesis.

**REFERENCES**

[1] Suresh, S. and Mortensen, A. (1998), *Fundamentals of Functionally Graded Materials*, IOM Communications Limited, London, UK.

[2] Paulino, G. H., Jin, Z. H. and Dodds Jr., R. H. (2003), "Failure of functionally graded materials", *Comprehensive Structural Integrity*, B. Karihallo and W.G. Knauss, eds., Elsevier Science, New York, Vol.2, chap. 13, pp. 607–644.

[3] Yildirm, B., Dag, S. and Erdogan, F. (2005), "Three dimensional analysis of FGM coatings under thermomechanical loading", *International Journal of Fracture*, Vol. 132, pp. 369-395.

[4] Elperin, T. and Rudin, G. (2002), "Thermal stresses in functionally graded materials caused by a laser thermal shock", *Heat and Mass Transfer*, Vol. 38, pp. 625-630.

[5] Saeedi, B., Sabour, A. and Khoddami, A.M. (2009), "Study of microstructure and thermal shock behavior of two types of thermal barrier coatings", *Materials and Corrosion*, Vol. 60, No.9, pp. 695-703.

[6] Nikolarakis, A. M., Theotokoglou, E. E. and Papathanasiou, T. K. (2013), "Finite element analysis of a functionally graded nickel-zirconia profile under thermal loading", *Proceedings of the 10th HSTAM International Congress on Mechanics,* Chania, Crete, Greece, 25-27 May 2013.

[7] Moler, C. B. (2008), *Numerical Computing with MATLAB*, 2nd Edition, Society for Industrial and Applied Mathematics, USA.

[8] Nowacki, W. (1986), *Thermoelasticity*, PWN - Polish Scientific Publishers, Warszawa.

[9] Hughes, T. J. R. (1987), *The Finite Element Method, Linear Static and Dynamic Finite Element Analysis*, Prentice Hall, Inc., New Jersey.

[10] Butcher, J. C. (2008), *Numerical Methods for Ordinary Differential Equations*, John Wiley & Sons Ltd, The Atrium, Southern Gate, Chichester, West Sussex PO19 8SQ, England.

[11] Joshi, S. C. and Ng, H. W. (2011), "Optimizing functionally graded nickel-zirconia coating profiles for thermal stress relaxation", *Simulation Modelling Practice and Theory*, Vol. 19, pp. 586-598.

[12] Zaki, M., Tarlochan, F. and Ramesh, S. (2013), "Two dimensional elastic deformations of functionally graded coated plates with clamped edges", *Composites: Part B*, Vol. 45, pp. 1010-1022.